Shape and size of simple cations in aqueous solutions: A theoretical reexamination of the hydrated ion via computer simulations

José M. Martínez, Rafael R. Pappalardo, and Enrique Sánchez Marcos[a)]
Departamento de Química Física, Universidad de Sevilla, 41012 Sevilla, Spain

The simplest representation of monoatomic cations in aqueous solutions by means of a sphere with a radius chosen on the basis of a well-defined property (that of the bare ion or its hydrate) is reexamined considering classical molecular dynamics simulations. Two charged sphere–water interaction potentials were employed to mimic the bare and hydrated cation in a sample of 512 water molecules. Short-range interactions of trivalent cations were described by Lennard-Jones potentials which were fitted from *ab initio* calculations. Five statistically independent runs of 150 ps for each of the trivalent spheres in water were carried out in the microcanonical ensemble. A comparison of structural and dynamical properties of these simple ion models in solution with those of a system containing the Cr^{3+} hydrate ($[Cr(H_2O)_6]^{3+}$) is made to get insight into the size and shape definition of simple ions in water, especially those that are highly charged. Advantages and shortcomings of using simple spherical approaches are discussed on the basis of reference calculations performed with a more rigorous hydrated ion model [J. Phys. Chem. B **102**, 3272 (1998)]. The importance of nonspherical shape for the hydrate of highly charged ions is stressed and it is paradoxically shown that when spherical shape is retained, the big sphere representing the hydrate leads to results of ionic solution worse than those obtained with the small sphere. A low-cost method to generate hydrated ion–water interaction potentials taking into account the shape of the ionic aggregate is proposed. © *1999 American Institute of Physics.* [S0021-9606(99)51703-0]

I. INTRODUCTION

Ionic solvation of monoatomic ions has long been understood in its energetic, structural and dynamical aspects on the basis of three landmark classical developments: the Born theory, the Debye–Hückel, and Debye–Hückel–Onsager theories.[1] They supply a simple and elegant model for ionic solutions allowing fruitful applications in multitude of physicochemical frameworks where ions in solution are involved. It is generally accepted that the simplicity of its formulation, only a few system-dependent parameters are needed (e.g., ion charge, dielectric permittivity of the solvent and ionic radius, when applied), is certainly one of the keys of their success. The phenomenological factors usually added to these models in order to fit to experimental results cannot hide that these crude theories retain some of the main features of the ion solvation.[2–4] Although these theories come from the 1920s, the recent improvements in quantum and statistical mechanics of condensed medium have compelled different authors to get insights into the microscopical interpretation of the parameters. Their aim has been to develop new concepts for a better understanding in the molecular basis of these theories.[2,5,6] A common feature of these models is the spherical shape adopted for the ions in solution, a feature that may easily be accepted for the case of simple monoatomic ions. To get fair agreement with experimental data, the most frequently altered parameter is the radius, as shown by Latimer *et al.* in their early study.[7] Within this line an important activity has appeared during the last ten years

to suggest a physically meaningful set of radii for simple ions.[8,9] Nowadays, computer simulations are providing a crucial bridge between general theories of solution and the microscopical level of the studied system, as they allow a large number of numerical experiments which test the main basis and trends classically pointed out by the pioneer theories of electrolyte solutions.[10–14]

A chemical concept coming from early studies of ionic solutions was that of the hydrated ion. This concept recognizes that some ions, mainly metallic and highly charged cations, in aqueous solutions behave as more complex entities than expected. The aggregate formed by the ion and a given number of solvent molecules surrounding it $[M(H_2O)_m]^{n+}$, was called the hydrated ion. It could explain physicochemical properties whose observed values cannot be easily understood on the basis of simple bare ions, M^{n+}.[15] Our group has used this concept within the framework of computer simulations of ionic solutions. The implementation of this old electrochemical concept within statistical simulations has been performed by developing an ion–water interaction potential, where the ion is present in its most stable hydrated form, $[M(H_2O)_m]^{n+}$. Thus, an *ab initio* $[Zn(H_2O)_6]^{2+}$-H_2O intermolecular potential was first developed and tested by Monte Carlo (MC) simulations of the Zn^{2+} hydration.[16] This potential has been called HIW (hydrated ion-water). Further MC and molecular dynamics (MD) simulations not only with Zn^{2+},[17] but also on the more involved Cr^{3+} hydration,[18,19] have been promising, since they have simultaneously supplied satisfactory results for energetic, structural, and dynamical properties, without the in-

―――――――――――――――
a)Electronic mail: sanchez@mozart.us.es
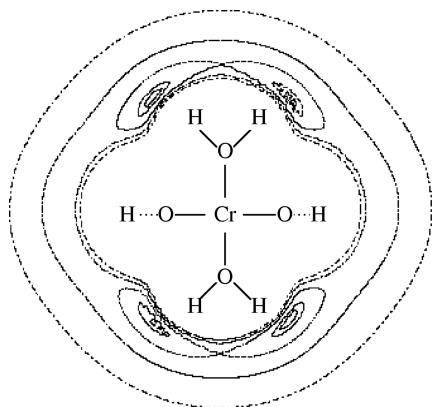
Scheme 1. Isoenergy curves corresponding to the most favorable interaction of a probe H_2O with the Cr^{3+} hexahydrate.

Scheme 2. Representation of the three trivalent cation models interacting with water molecules: HI (top), Q3S (left-hand side), and Q3B (bottom).

clusion of any kind of empirical parameters in the proposed potentials. Likewise, several authors have recently used the hydrated ion concept to develop, in different ways, intermolecular interaction potentials of metal cations.[20–25] Their results also point out the advantages of this approach to describe a wide set of physicochemical properties of ionic solutions.

Our analytical potential, developed for the hydrated ion–water interactions, precisely describes the shape of this cluster. Scheme 1 shows a two-dimensional map of isoenergetic curves corresponding to the most favorable interaction between the $[Cr(H_2O)_6]^{3+}$ and a probe water molecule.[18,19(a)] The drawn plane is that containing the cation and four oxygen atoms. It is seen that although at long distances the isolines are almost circular, at short distances they follow the molecular shape of the hydrate. Scheme 1 compelled us to undertake a new study examining how changes of the shape and size for these metal ions affect the properties of ionic solutions, particularly the less studied dynamical properties. To achieve this goal, the results of simulations of two simple spherical models for a trivalent cation will be compared with those previously obtained for the Cr^{3+} hydrate.[19(a)] For the first trivalent charged sphere, the radius is chosen such that the bare ion is mimicked, whereas in the second case the radius value corresponds to that derived from a hydrated ion (Scheme 2). The former model will be called Q3S (charge +3 small) and the particle will have a mass equal to that of the chromium atom. The latter model will be called Q3B (charge +3 big) and since it is a crude representation of the hydrated ion, the mass assigned will be that of the Cr^{3+} hexahydrate. When generating the interaction potentials of these spheres with water molecules, special attention was paid to using criteria that did not introduce significant differences with respect to the HIW potential of the Cr^{3+}, apart from the intrinsic topological ones. It is worth pointing out that the objective of these two new simple potentials is not to improve the well-tested representation given by the HIW potential,[18,19] but rather to get insights into basic factors controlling the interparticle forces in ionic solutions.
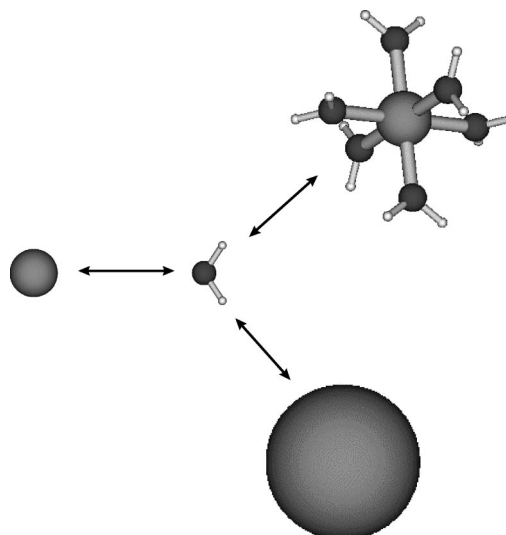
II. METHODOLOGY

A. Intermolecular potentials.

The $[Cr(H_2O)_6]^{3+}$–H_2O intermolecular potential has already been described elsewhere.[18,19(a)] The general expression for this HIW potential is

$$E_{HIW} = \sum_i^{HI\ sites} \sum_j^{W\ sites} \left(\frac{C_4^{ij}}{r_{ij}^4} + \frac{C_6^{ij}}{r_{ij}^6} + \frac{C_{12}^{ij}}{r_{ij}^{12}} + \frac{q_i q_j}{r_{ij}} \right), \qquad (1)$$

where indices i,j run over the sites of the HI and water molecule, respectively.

Q3S– and Q3B–water interaction potentials (Q3XW, X=S,B) have been defined by means of a Lennard-Jones plus a Coulombic term:

$$E_{Q3XW} = 4\epsilon \left[\left(\frac{\sigma}{r_{QO}} \right)^{12} - \left(\frac{\sigma}{r_{QO}} \right)^6 \right] + \sum_j^{W\ sites} \frac{q_Q q_j}{r_{Qj}}, \qquad (2)$$

where $q_Q = +3$. σ values (1.825 and 3.625 Å for Q3SW and Q3BW, respectively) were chosen in such a way that they led to minimum values in the Lennard-Jones part of the Q3SW and Q3BW interaction curves at the same ion–oxygen distances than those characteristic of computations of Cr^{3+} in water. Thus, for the small sphere the *ab initio* Cr-O_I distance in the hexahydrate (2.05 Å),[18] and for the big sphere the first maximum of the g_{Cr-O} for the previous Cr^{3+} hexahydrate simulation (which corresponds to an ion–second–shell distance, Cr-O_{II}=4.06 Å[18]), were the applied criteria. Figure 1 shows the Lennard-Jones curves for both charged soft spheres. ϵ values (426.7626 and 52.1092 kJ mol^{-1} for Q3SW and Q3BW, respectively) were obtained from the Hartree–Fock interaction energy of a triple charge point and a TIP4P-geometry water molecule at the previously mentioned distances. From the total interaction energy, the electrostatic part is subtracted. Basis sets for the water molecule were the same as those used in the development of the HIW interaction potential.[18] For the sake of comparison, the interaction energy corresponding to the optimized arrangement of a water molecule around the HI and Q3B has been calculated, its
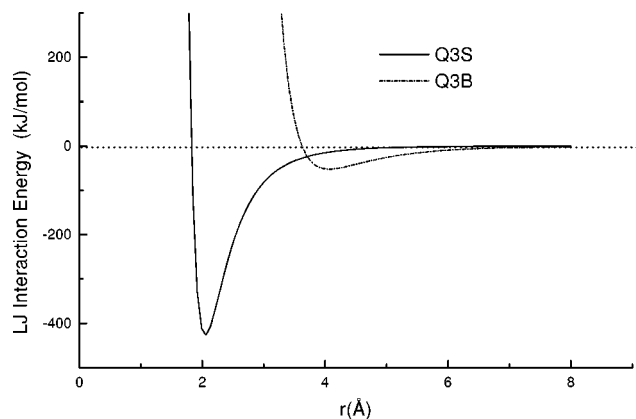
FIG. 1. Lennard-Jones curves for water–soft spheres interaction energies.

FIG. 2. Ion–oxygen (a) and ion–hydrogen (b) RDFs for the different simulations.

value being −149.6 and −160.9 kJ mol^{-1}, respectively. The similarity of these two quantities means that the Q3BW potential model has primary ion–water interactions in the second shell region close to that of the more refined HIW potential.

B. MD simulation details

Molecular dynamic simulations were performed in the NVE ensemble using periodic boundary conditions. The system was formed by the corresponding charged sphere plus 512 H$_2$O which were described by the TIP4P model.[26] The ion–water interactions were described by the two previously presented potentials: Q3SW and Q3BW. The basic cell was a cubic box with 24.8 Å per side. Simulations were run with the MOLDY program[27] (version 2.10). Newton–Euler equations of motion were integrated using a modified form of the Beeman algorithm[28,29] which guarantees a good stability for molecular systems. Orientations of solvent molecules, which were assumed to be rigid, were described by the quaternion formalism.[30] The time step employed was 0.3 fs in order to avoid energy drift.

Coulombic interactions were computed using the Ewald sum technique,[31] including the charged system term.[32] Although this treatment is costly, the importance of its use to obtain reliable structural and, particularly, dynamical results in the case of ionic aqueous solutions, has been shown.[32–34] A spherical molecular cutoff was applied to the real space part of the Ewald energy as well as the short-range potential, which were treated by an implementation of the link cell method.[35,36] Corrections to the potential energy and pressure arising from the use of the cutoff were included.

Thermalization time was about 40 ps and temperature was 298 K along the simulation. For each system the total simulation time was 750 ps divided into 5 statistically independent runs of 150 ps. To achieve such condition, a small reequilibration period was applied between subsequent runs of the simulated system. Trajectories and velocities were collected every 40 time steps. Computations were carried out on a parallel HP X-CLASS SPP-2000 Series where an efficient parallelization of the program was obtained.
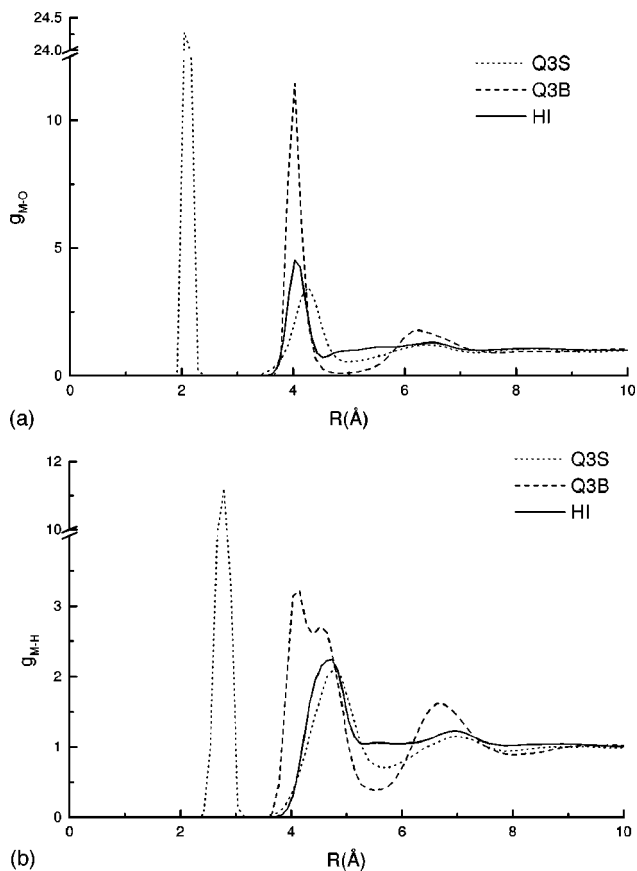
III. RESULTS

A. Structural results

Preliminary structural results of the charged spheres in water derived from simulations with shorter running time have already been presented elsewhere.[19(a)] Analyses do not change significantly for longer simulation times, so that in this section we will summarize the more important results, in order to help in understanding the dynamical results presented below. Figure 2 shows the RDF (radial distribution function) for ion–oxygen (a) and ion-hydrogen (b) pairs obtained with the two charged spheres and the hydrated ion model. According to definitions, only the Q3S simulation gives information on the first shell. Maxima for the first Q3S–O and Q3S–H peaks are centered at 2.05 and 2.75 Å, respectively, and integrates to 9 water molecules. This overestimation has been previously reported in simulations of ionic solutions[37] and attributed to large many-body effects.[38] The peaks corresponding to the second hydration shell are centered at 4.26 Å (Q3S–O RDF), 4.02 Å (Q3B–O RDF), and 4.07 Å (HI–O RDF) and integrates to 18 (Q3S–O), 25 (Q3B–O), and 14 (HI–O) oxygen atoms. Cation-hydrogen RDF for the solution containing Q3S presents a wide peak corresponding to the second shell centered at 4.8 Å (the integration number is 44), the Q3B presents a wide double peak at 4–5 Å which integrates to ~55 hydrogen atoms, and the HI presents a wide peak centered at 4.65 Å (the integration number is ~32).
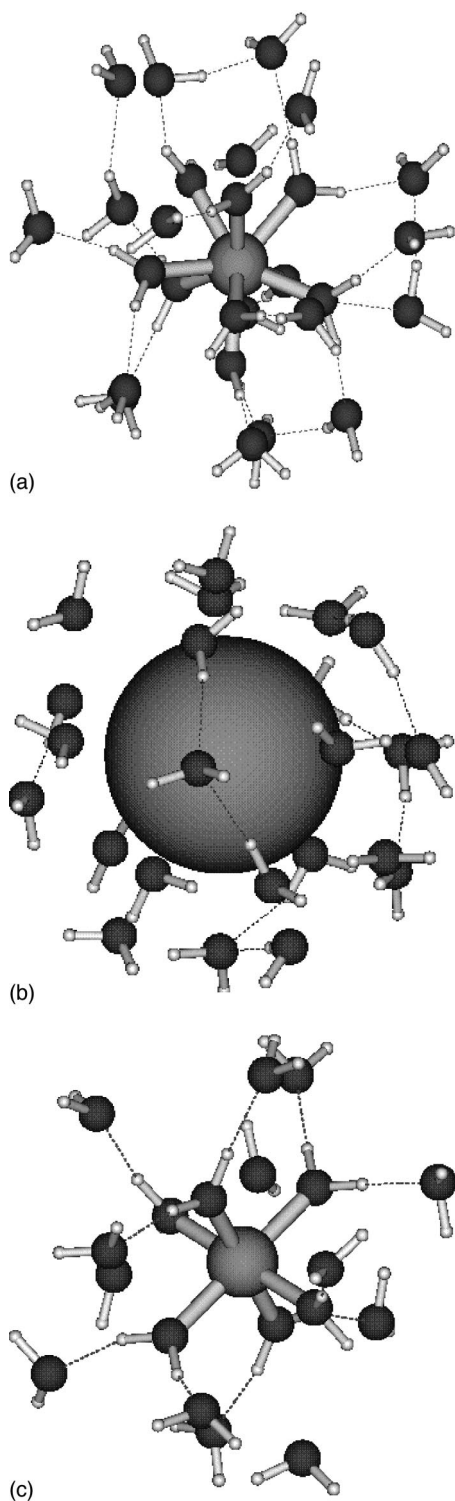
(a)

(b)

(c)

FIG. 3. Random snapshots taken from simulations containing the ions Q3S (a), Q3B (b), and HI (c), where the ion environment can be observed.

To visualize the type of arrangement around the charged spheres, random, but representative, configurations taken from the production period of Q3S and Q3B simulations are presented in Fig. 3,[39] together with a random configuration of the HI simulation. In the Q3B model [Fig. 3(b)] the hydration number for the second shell is largely overestimated (∼25), water molecules do not orientate their dipole moment vectors toward the cation, which explains the double peak

shown by the Q3B–H RDF [Fig. 2(b)]. The hydration structure adopted is close to those of clathrates of alkali metal cations, as suggested by looking at Fig. 3(b).[40] This means that the concurrence in Q3BW of an isotropic and damped (second-shell) interaction potential prevents an extensive breaking of the water structure around Q3B. The absence of preferential interaction sites in Q3B allows the retention of a part of the water–water interactions taking place in the bulk. On the contrary, Q3S is surrounded by two quite well-defined hydration shells, where the 18 molecules of the second shell bound by pairs the 9 first-shell water molecules [Fig. 3(a)]. This is to say, though overestimated, specific interactions between the first and second shells define a number of preferential binding sites in the second-shell region which are responsible of the highly cation-oriented water structure. However, due to the overestimation of the first-shell hydration number, the structural error is propagated to the second shell. The hydrated ion approach supplies a fair ordering of solvent structure at the second-shell region on the basis that a correct hydration number for the first shell is previously imposed by the model [Fig. 3(c)].

B. Dynamical results

Translational self-diffusion coefficients, D, which describe the mobility of the charged spheres have been calculated by the mean-square displacement (MSD) method. The values obtained and that of the Cr^{3+} hydrate previously obtained under similar conditions[19(a)] are:

$$HI: (0.68 \pm 0.16) \times 10^{-5} \ cm^2 \ s^{-1},$$

$$Q3S: (0.74 \pm 0.15) \times 10^{-5} \ cm^2 \ s^{-1},$$

$$Q3B: (0.43 \pm 0.09) \times 10^{-5} \ cm^2 \ s^{-1}.$$

Likewise, the computation of these coefficients from the velocity autocorrelation function (VACF) yields values for D which are the same within the uncertainty degree of these estimates. Therefore, from the three models employed to represent the Cr^{3+} cation, the big sphere is the particle with a smaller mobility, whereas the small sphere and the hydrated ion show statistically equivalent mobilities.

Contrary to structural and energetical information,[6,12,13,41] there is scarce detailed comparison on the dynamical behavior of single ions as a function of the radius size for spheres[4(a),11,42] and, in case a hydrate is recognized, as a function of the shape. The basic question at the dynamical level that may be proposed refers to the influence that these two basic features have on the ionic mobility. At first sight, two opposite causes may be invoked to help in predicting the possible D sequence. On the one hand, if ion size was the dominant factor, it would lead to displacements for Q3B and HI, which have the same mass (160 amu) but different shape, more greatly hindered than for the much smaller Q3S, whose mass is that of the cation (52 amu), i.e., $D_{Q3B} \approx D_{HI} < D_{Q3S}$. On the other hand, if ion–water interactions were the dominant factor, then they would be stronger for Q3S than for Q3B and HI in a twofold sense: First, the Q3SW potential includes interactions of the ion with first-shell water molecules, and second, this potential implicitly

overestimates interactions due to many-body terms, so the expected sequence would be $D_{Q3B} \approx D_{HI} > D_{Q3S}$. However, the sequence obtained is neither of them, but rather a compromise among these two factors and an additional one: water–water interactions among the molecules forming the close environment of Q3S (the first hydration shell) as well as their interaction with outer solvation shells. In this sense, Lee and Rasaiah[11] have recently shown by MD simulations how is possible to reproduce the observed maximum in the mobilities of alkaline cations in water as a function of size and interaction energies, Rb^+ being the cation with the highest mobility along the series Li^+–Cs^+.

As shown in the structural analysis of Q3S–O and Q3S–H RDFs, and it is now found again in the dynamical results, that Q3S goes through solution surrounded by a tight first shell of solvent molecules. In this sense, the small size of Q3S must be understood on the basis that the particle to which its mobility is calculated is a sphere having a triple charge and the mass of the chromium atom. However, the strong interactions with its first shell of water molecules forces Q3S to move through the solution with such a solvent cosphere attached. This is also the case of the HI, where *a priori* a first shell is imposed by the model, but in this case 6 instead of 9 solvent molecules accompany the trivalent cation. According to these hydration numbers, one could expect that Q3S moved slower than HI. However, since the water model employed is not polarizable, interactions between the first and second hydration shells for the HI simulation are stronger than for the Q3S simulation. When building the HIW potential,[18] the first-shell water molecules are polarized because quantum chemical calculations dealt with $[Cr(H_2O)_6]^{3+}$. However, in the Q3S simulation, the 9 solvent molecules forming the first shell bear the charge distribution of a TIP4P H_2O. To check this point the maximum interaction energy of a TIP4P water molecule with the $[Q3S(H_2O)_9]^{3+}$ aggregate is -113 kJ/mol. This value is smaller than the corresponding value for HI (-149.6 kJ/mol). The structural information goes in the same way: The distance between the ion and the oxygen of the molecule interacting with the aggregate is 4.16 and 4.11 Å for Q3S and HI, respectively. Therefore, both results show that interactions between the first and second shells are stronger in the case of the HI model and those should operate in hindering the mobility of the cation. In this sense, it may be concluded that a substantial cancellation of effects takes place in the D_{Q3S} value, due to the opposite behavior that this magnitude has on the many-body terms, leading to a $n_h = 9$, and the TIP4P model of nonpolarizable water.

Let us analyze the result for the big sphere, Q3B. The structural information given by Q3B–O and Q3B–H RDFs shows a picture that is far from simple, as derived from the peculiar structure adopted by the second hydration shell [Fig. 3(b)]. The clathratelike structure found for the ensemble of water molecules around the big sphere hinders the mobility of the cation in such degree that its D_{Q3B} value becomes the smallest one of those studied.

An additional dynamical magnitude describing the environment of the ion is the mean residence time (MRT) of water molecules inside the second hydration shell. Calcula-

TABLE I. Mean residence time (ps) of water molecules in the second hydration shell of the different types of trivalent cation model. (For definition of t^* see the text.)

	Cation model		
t^*	Q3S	Q3B	HI
0	4.7 ± 0.6	23 ± 3	6 ± 1
2	20 ± 2	55 ± 6	32 ± 5

tions have been carried out applying Impey *et al.*'s method[43] in the same way as in the previous study of the Cr^{3+} hydrate in water.[19(a)] Thus, two values for t^*, 0 and 2 ps, have been used aiming to establish a MRT range of values that accounts reasonably for this magnitude. Table 1 collects the results for the two charged spheres and for the Cr^{3+} hydrate. Analysis of these data indicates that the persistence of water molecules in the second shell is quite similar for the simulations of Q3S and HI, whereas that of Q3B MRTs are longer. This is a consequence of the peculiar clathrate structure adopted by water molecules around the big sphere, reflecting the persistence of a well-defined water environment when comparing with Q3S and HI solutions. Likewise, a reexamination of M–O and M–H RDFs (Fig. 2) shows that the largest decay in the second–third shell transition region is found for Q3B. This feature agrees with the dynamical behavior of the ion as well as with the MRT computed for the second-hydration-shell water molecules. The large second-shell water molecules' MRT values in the Q3B simulation, joined to the previous structural information allows an additional physical foundation to understand the smallest mobility of the big sphere. Although the dynamical behavior is obtained by analyzing one sphere with the mass of the Cr^{3+} hexahydrate, a significant part of the molecules forming the second shell accompany the Q3B during its motion. Thus, the actual diffusing object becomes larger than the corresponding ionic entities moving through the Q3S and HI solutions.

IV. DISCUSSION

The tight binding of water molecules around cation has long been invoked, in particular for highly charged ones, to justify the ascription of an ionic radius much larger than that expected from its electronic structure. The most common frame where this idea has been used, assumed a simple representation of the solvent as a polarizable dielectric continuum or an ensemble of hard or soft spheres. The dynamical results presented here show that the use of a big and uniformly charged sphere does not give a reasonable representation when describing the mobility of a hydrated ion in a *solvent described at the microscopical level*.

The standard Born radii are in fact parameters which try the minimization of two important shortcomings of the Born equation: the continuum representation of the solvent (in our case water) and the use of an unique dielectric permittivity value for this polarized continuum.[7,15] When a discrete representation of the solvent is used, the dielectric response to the high electric field defined by ions in solution is implicit in the microscopical description of the solvent and in the

interparticle forces defined in the system. The local dielectric response is of particular importance in the close environment of the triple charge, given that dielectric decrement phenomena appear to a large extent.[44]

It is worth commenting on the dielectric screening associated with the three different models of trivalent cation employed in this study. For the HI model, the first-shell water molecules have been quantum-mechanically described within the hydrate. Thus electronic and nuclear polarization, as well as partial charge transfer effects are collected in these molecules and are responsible for important screening effects on the rest of solvent molecules. Additionally, screening effects are implicit in the HIW potential given that the fitted energies for hydrate–water interactions come from *ab initio* calculations where the test water molecule is polarized as a function of the orientation and distance to the hydrate. For the case of the two spheres, the only type of water molecule present is TIP4P, so that mainly indirect dielectric screening effects are present. These indirect effects have a twofold origin. The first one is the *ab initio* interaction energy which accounts for the electronic polarization of the test water molecule, as previously mentioned in the case of the HIW potential. The second origin is the *a priori* definition of the optimum ion–water distance, that is external data reflecting in some way direct interactions among the ion and its first two hydration shells. Since the importance of the local dielectric response in the first hydration shell has long been recognized,[45] results for the Q3B model may be understood, in part, on the basis of an insufficient local dielectric response within this model. The big sphere shows to the solution an homogeneous surface that allows to the closer water molecules a certain degree of freedom to improve their interactions with neighboring water molecules more easily than if the first shell ion showed specific interactions sites. The solvent molecules forming the first hydration shell of Q3S make possible the presence of such specific sites and then, the Q3SW potential includes implicitly some dielectric screening effects in the first shell. Therefore, the hydration model for Q3S is an intermediate situation between those of HI and Q3B. The ensemble of structural and dynamical results reinforces the previous conclusion given by Hyun *et al.*[10] on the critical importance of noncontinuum behavior of the structure of the solvent in the first shell to reach reasonable estimates of the ion solvation energy.

Our results suggest the intriguing paradox that the trial of using a big sphere for a highly charged ion in a solvent described at the molecular level leads to a description of the solution even worse than that derived from the use of the intrinsic ionic radius (bare ion). Bearing in mind the precedent discussion, this may be ascribed to the fact that the representation of the solute and the solvent is unbalanced. The paradoxical fact is that it was just to describe hydration phenomena of transition metal and highly charged ions, such as Cr^{3+}, Rh^{3+}, Al^{3+}, Cu^{2+}, etc., where the use of the hydrated ion concept was more widespread.[7,9,15] As a consequence, these cases were the pattern taken to associate ions in solution with big spheres of effective (and large) radii. Based on the divergent results obtained with the use of Q3B and the HI model (Scheme 1), in addition to the weakness of
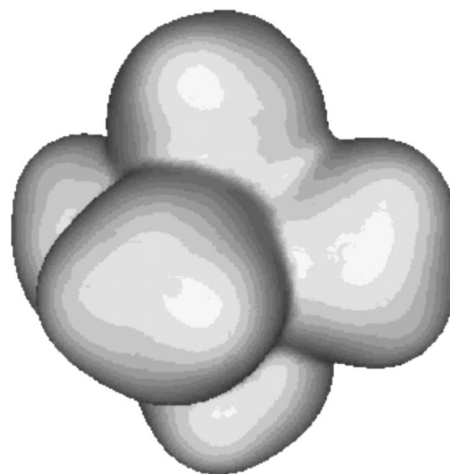

FIG. 4. Isodensity surface of the Cr^{3+} hexahydrate.

the Q3B model related to the poor local dielectric response, a new factor seems to get relevance: the shape of the aggregate in solution. Thus, the shape of the hydrated ion, as shown in Fig. 4 for the Cr^{3+} hexahydrate, is quite different from a sphere. When dynamic properties are evaluated the shape appears as a crucial factor. This is confirmed by the results obtained for the small sphere model which, though limited by strong many-body effects, is able to fix tightly solvent molecules around it and impose a more adequate order to the outer solvent structure. Short-range anisotropy implicit in the first-shell region is a key point for a correct description of a single highly charged cation. In this sense, it is understandable that these types of cations are neither so simple nor really spherical in aqueous solutions.

From this conclusion a strategy to build a low-cost hydrated ion potential (LCHIW) may be envisaged: the geometry of the LCHI is the same as the HI; the Non-Coulombic interaction between the first-shell water molecules and those of the bulk are described by the TIP4P potential; electrostatic charges are those of the HIW potential and the chromium ion is only involved in the Coulombic term of the potential. This procedure of obtaining the interaction potential saves the large number of quantum mechanical computations ($\sim$1200) which are needed to build the HIW potential,[16,18] and the fit of the *ab initio* interaction energies to a suitable functional form. In this sense, the term ''low-cost'' may be justified, as LCHIW only needs the quantum mechanical optimization of the hydrated ion plus a fitting of the effective charges on the cluster atoms in order to reproduce the electrostatic potential generated by the molecular wave function. RDFs derived from a MD simulation (150 ps run under the same conditions as the rest of presented simulations) of such a kind of hydrated ion plus 512 H_2O are shown in Fig. 5 together with the distributions obtained for the Q3S model. These results show the correct trend in predicting the position of the peaks for the second hydration shell as well as in the integration number. The key feature of a well-behaved potential is then a well shape-adapted and charge-distributed description for the ion and its close environment.

Bearing in mind this discussion, the following two main remarks may be concluded.
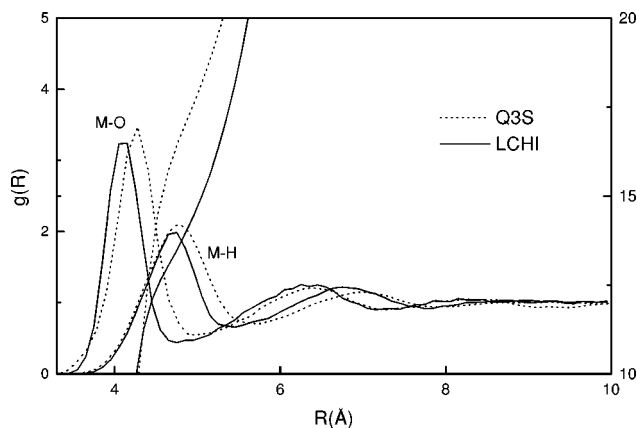
FIG. 5. Ion–oxygen and ion–hydrogen RDFs for the simulations containing the low-cost hydrated ion (LCHI) and the small charged sphere (Q3S).

(1) The description of highly charged ions in water and other polar solvents based on theory of solutions might be improved if shapes fitting the solvated ion are considered. In this sense, general continuum solvation models such as that of Tomasi's group (PCM model)[46] retains this property. Likewise, Rick and Berne in the simple case of the aqueous solvation of water also conclude the importance of the solute's shape when comparing a continuum method with MD simulations.[47]

(2) From computer simulations, practical ways might be envisaged to introduce the anisotropy of solvated ions by means of the inclusion of restrictions to a given number of solvent molecules surrounding the ion. Even though the short-range potential of these solvent molecules is not an ''ad hoc'' one, it will improve the description of the solvation phenomenon. Merbach *et al.*[20] have recently adopted this type of strategy and found quite satisfactory results. This low-cost line of procedure may be of particular relevance when dealing with salt effects on biomolecules of medium and large sizes.[3] These types of potentials, on the one hand guarantee a fair description of interaction energies once eliminated from the largest part of many-body terms, and on the other hand, prevent uncontrolled dehydration phenomena and collapse of biomolecule three-dimensional structures.

ACKNOWLEDGMENTS

[1] (a) M. Born, Z. Phys. **1**, 45 (1920); (b) P. Debye and E. Hückel, *ibid.* **24**, 185 (1923); (c) L. Onsager, *ibid.* **28**, 277 (1927); (d) R. M. Fuoss and L. Onsager, J. Phys. Chem. **66**, 1722 (1962).

[2] B. Roux, H.-A. Yu, and M. Karplus, J. Phys. Chem. **94**, 4683 (1990).

[3] B. Honig and A. Nicholls, Science **268**, 1144 (1995).

[4] (a) P. G. Wolynes, Annu. Rev. Phys. Chem. **31**, 345 (1980); (b) J. Hubbard and P. G. Wolynes, in *The Chemical Physics of Ion Solvation*, edited by R. R. Dogonadze, E. Kalman, A. A. Kornyshev, and J. Ulstrup (Elsevier, Amsterdam, 1985), Pt. C, Chap. 1.

[5] P. G. Wolynes, J. Chem. Phys. **68**, 473 (1978).

[6] J.-K. Hyun and T. Ichiye, J. Phys. Chem. **101**, 3596 (1997).

[7] W. M. Latimer, K. S. Pitzer, and C. M. Slansky, J. Chem. Phys. **7**, 108 (1939).

[8] A. A. Rashin and B. Honig, J. Phys. Chem. **89**, 5588 (1985).

[9] Y. Marcus, Chem. Rev. **88**, 1475 (1988).

[10] J.-K. Hyun, C. S. Babu, and T. Ichiye, J. Phys. Chem. **99**, 5187 (1995).

[11] S. H. Lee and J. C. Rasaiah, J. Phys. Chem. **100**, 1420 (1996).

[12] (a) G. Hummer, L. W. Pratt, and A. E. García, J. Phys. Chem. **100**, 1206 (1996); (b) J. Chem. Phys. **107**, 9275 (1997).

[13] R. M. Lynden-Bell and J. C. Rassaiah, J. Chem. Phys. **107**, 1981 (1997).

[14] F. Figueirido, G. S. Del Buono, and R. M. Levy, J. Phys. Chem. **101**, 5622 (1997).

[15] (a) R. R. Robinson and R. H. Stokes, *Electrolyte Solutions*, 2nd ed. (Butterworths, London, 1959); (b) J. O.'M. Bockris and A. K. N. Reddy, *Modern Electrochemistry* (Plenum, New York, 1973), Vol. 1.

[16] R. R. Pappalardo and E. Sánchez Marcos, J. Phys. Chem. **97**, 4500 (1993).

[17] (a) E. Sánchez Marcos, J. M. Martínez, and R. R. Pappalardo, J. Chem. Phys. **105**, 5968 (1996); (b) , **108**, 1752 (1998).

[18] R. R. Pappalardo, J. M. Martínez, and E. Sánchez Marcos, J. Phys. Chem. **100**, 11748 (1996).

[19] (a) J. M. Martínez, R. R. Pappalardo, E. Sánchez Marcos, K. Refson, S. Díaz-Moreno, and A. Muñoz-Páez, J. Phys. Chem. B **102**, 3272 (1998); (b) J. M. Martínez, R. R. Pappalardo, and E. Sánchez Marcos, J. Chem. Phys. **109**, 1445 (1998).

[20] A. Bleuzen, F. Foglia, E. Furet, L. Helm, A. E. Merbach, and J. Weber, J. Am. Chem. Soc. **118**, 12777 (1996).

[21] E. Wasserman, J. R. Rustad, and S. S. Xantheas, J. Chem. Phys. **106**, 9769 (1997).

[22] (a) X. Periole, D. Allouche, J. P. Daudey, and Y. H. Sanejouand, J. Phys. Chem. B **101**, 5018 (1997); (b) X. Periole, D. Allouche, A. Ramírez-Solís, I. Ortega-Blake, J. P. Daudey, and Y. H. Sanejouand, *ibid.* **102**, 8579 (1998).

[23] (a) F. Floris, M. Persico, A. Tani, and J. Tomasi, Chem. Phys. Lett. **199**, 518 (1992); (b) Chem. Phys. **195**, 207 (1995).

[24] M. N. D. S. Cordeiro and J. A. N. F. Gomes, J. Comput. Chem. **14**, 629 (1993).

[25] A. P. Lyubartsev and A. Laaksonen, Phys. Rev. E **55**, 5689 (1997).

[26] W. L. Jorgensen, R. W. Impey, J. Chandrasekhar, J. D. Madura, and M. L. Klein, J. Chem. Phys. **79**, 926 (1983).

[27] K. Refson, MOLDY *User's Manual Rev. 2.10* MOLDY code can be obtained from the CCP5 program library or by anonymous ftp from ftp.earth.ox-.ac.uk.

[28] D. Beeman, J. Comput. Phys. **20**, 130 (1976).

[29] K. Refson, Physica B & C **131**, 256 (1985).

[30] H. Goldstein, *Classical Mechanics*, 2nd ed. (Addison-Wesley, Reading, MA, 1980).

[31] M. P. Allen and D. J. Tildesley, *Computer Simulations of Liquids* (Oxford University Press, Oxford, 1987).

[32] J. E. Roberts and J. Schnitker, J. Phys. Chem. **99**, 1322 (1995).

[33] J. D. Madura and B. M. Pettitt, Chem. Phys. Lett. **150**, 105 (1988).

[34] L. Perera, U. Essmann, and M. L. Berowitz, J. Chem. Phys. **102**, 450 (1995).

[35] B. Quentrec and C. Brot, J. Comput. Phys. **13**, 430 (1975).

[36] D. W. Hermann, *Computer Simulation Methods*, 2nd ed. (Springer, Berlin, 1990).

[37] (a) M. M. Probst, E. Spohr, and K. Heinzinger, Chem. Phys. Lett. **161**, 405 (1989); (b) Mol. Simul. **7**, 43 (1991); (c) A. González-Lafont, J. M. Lluch, A. Oliva, and J. Bertrán, Chem. Phys. **111**, 241 (1987); (d) M. N. D. S. Cordeiro, J. A. N. F. Gomes, A. González-Lafont, J. M. Lluch, and J. Bertrán, *ibid.* **141**, 379 (1990).

[38] (a) L. A. Curtiss, J. W. Halley, J. Hautman, and A. Rahman, J. Chem. Phys. **86**, 2319 (1987); (b) N. J. Elrod and R. J. Saykally, Chem. Rev. **94**, 1975 (1994).

[39] G. Schaftenaar, MOLDEN: A portable Electron Density Program, QCPE Program 619; QCPE Bull. **12**, 3 (1992).

[40] (a) A. Selinger and A. W. Castleman, Jr., J. Chem. Phys. **95**, 8442 (1991); (b) J. Cioslowski and A. Nanayakkara, Int. J. Mod. Phys. B **23&24**, 3687 (1992); (c) J. Lipkowski, Annu. Rep. Prog. Chem., Sect. C: Phys. Chem. **92**, 307 (1996).

[41] M. I. Bernal-Uruchurtu and I. Ortega-Blake, J. Chem. Phys. **103**, 1588 (1995).

[42] Th. Kowall, F. Foglia, L. Helm, and A. E. Merbach, J. Am. Chem. Soc. **117**, 3790 (1995).

[43] (a) A. W. Impey, P. A. Madden, and I. R. McDonald, J. Phys. Chem. **87**, 5071 (1983); (b) A. E. García and L. Stiller, J. Comput. Chem. **14**, 1396 (1993).

[44] J. M. G. Barthel, H. Krienke, and W. Kunz, *Physical Chemistry of Electrolyte Solutions* (Springer, Darmstadt, 1998), p. 104.

[45] R. Pottel, in *Water. A Comprehensive Treatise*, edited by F. Franks (Plenum, New York, 1973), Vol. 3, Chap. 8.

[46] (a) S. Miertus, E. Scrocco, and J. Tomasi, Chem. Phys. **55**, 117 (1981); (b) S. Miertus and J. Tomasi *ibid.*, **65**, 239 (1982).

[47] S. W. Rick and B. J. Berne, J. Am. Chem. Soc. **116**, 3949 (1994).